Supplementary Materials

This supplementary file includes:

Figs. S1 to S7

Supplementary Table S1

Captions for movies S1 and S2

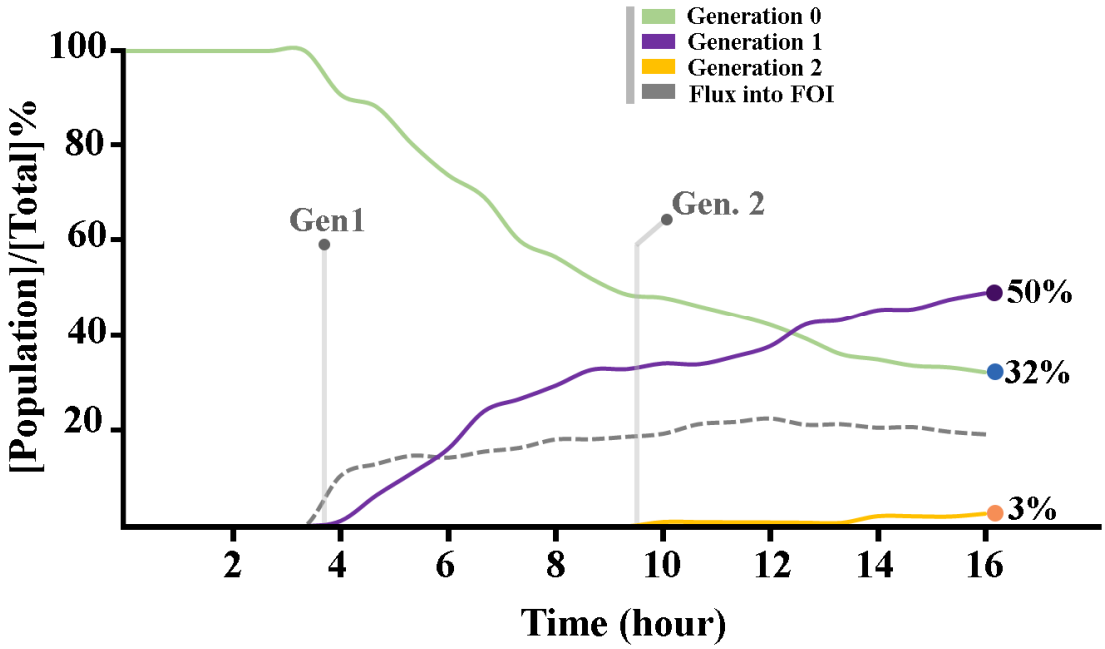

Fig. S1. Live-cell imaging analysis of cell division profile. Mitotic event were binned in 40-minute intervals where generations 1 refers to cells generated from generation 0. Cells in generation 2 were produced from generation 1. Flux into ROI (region of interest) shows the cells that migrate into ROI from the boundaries of ROI.

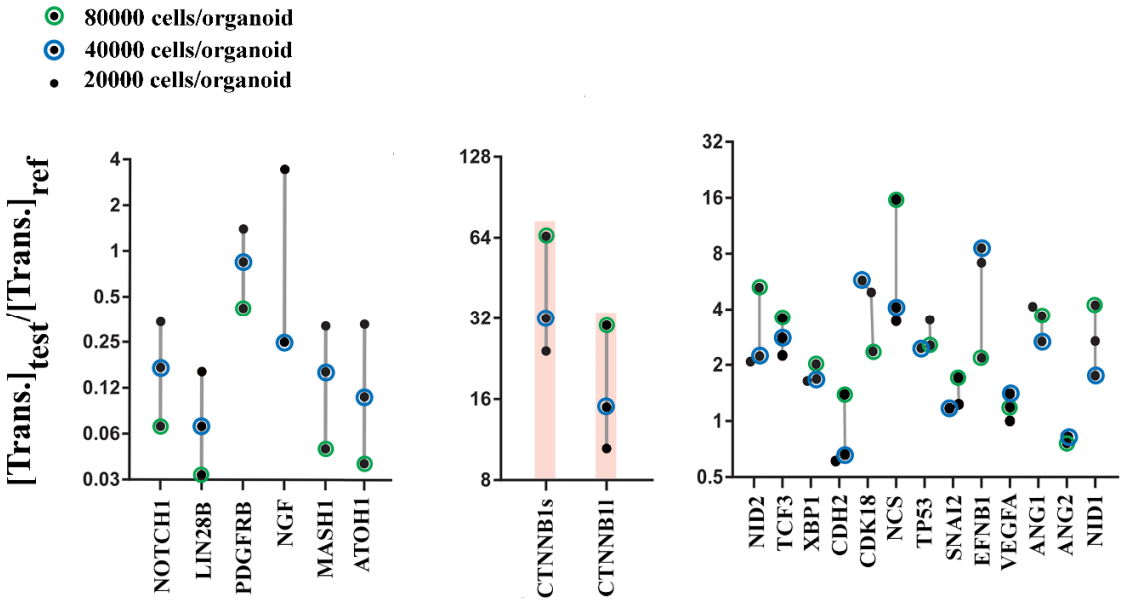

Fig. S2. Gene expression profiling of organoids that comprise increasing number of cells. Expression level are normalized to β-actin and referenced to organoids with 10000 cells. Note that the expression of majority of the genes does not reflect the organoid size (right panel). The expression of Notch cascade genes decreases proportional to the size of organoid (left panel). The expression of catenin-β1 (short (s) and long (l) isoforms) increases proportional to the number of cells in organoid (middle panel). As such, catenin-β1 has got the capacity to sense and respond to the density of cells in a population. In conditions of increased cell density, upregulation of catenin-β1 reduces the synchronization threshold of the population to limit the growth potential of organoids (quorum sensing activity).

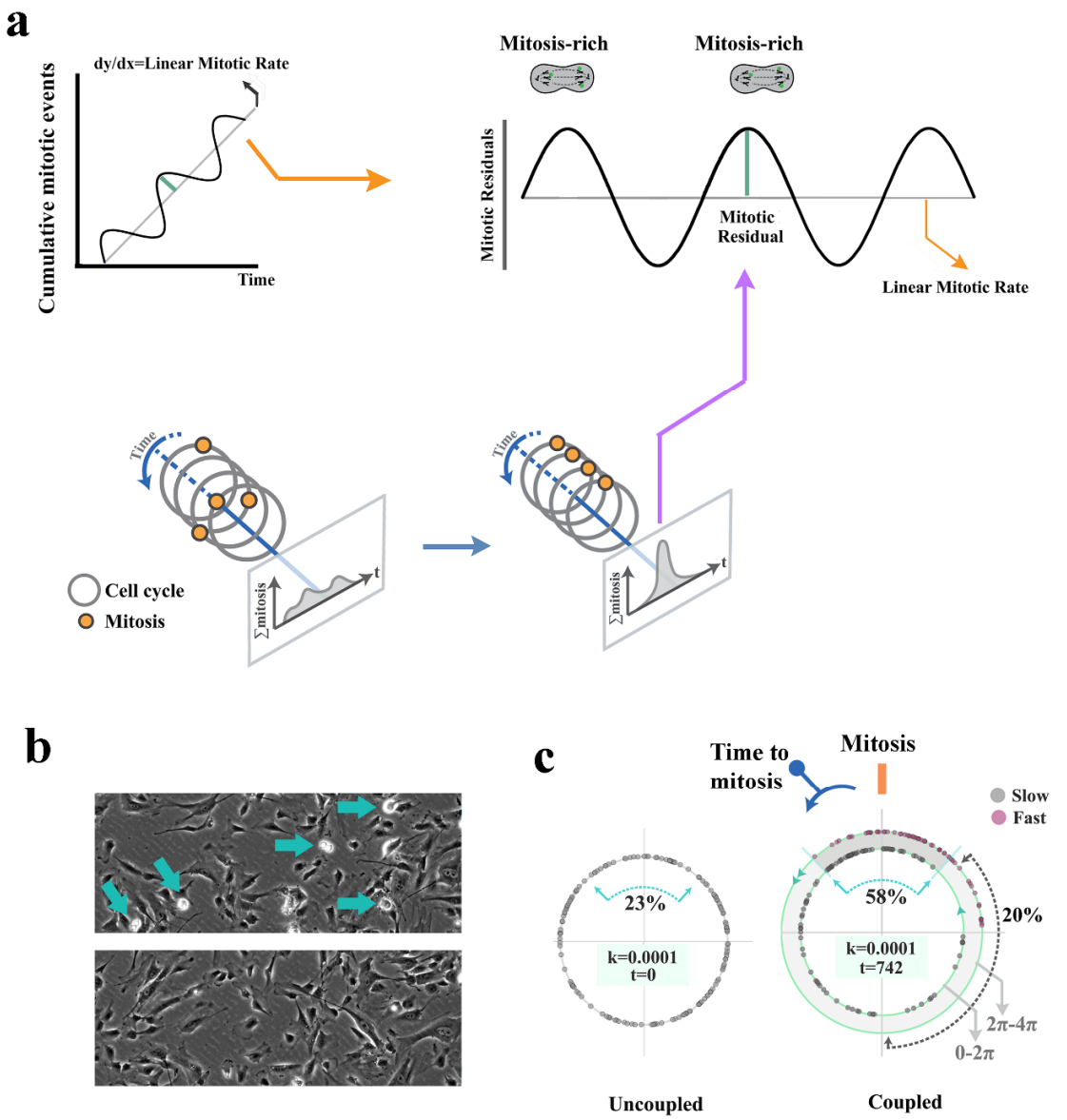

Fig. S3. Schematic demonstration of methods used for assessment of mitotic landscape. The black line (top left) shows cumulative incidence of mitotic events. The grey line (top left) shows a least-squares regression line fitted into the cumulative incidence graph. The slop of the least-squares regression line indicates linear mitotic rate. Positive and negative deviations from such linearity (residuals: green line) result from synchronous mitotic events followed by mitosis-poor periods when synchronized neural progenitors are collectively in the interphase. As such, amplitude of population-level mitotic oscillations reflects relative synchronization of the cycling cells. The right graph is a transformed version of the left one subsequent to counter-clockwise rotation of xy-Cartesian coordinate system to an x'y'-Cartesian coordinate system in which the x' parallel the least squares regression line. **b,** Phase contrast images show mitosis-rich (top, arrows) and mitosis-poor periods that reflect partial synchronicity of the population of progenitor cells. **c,** In order to model emergence of synchronicity by coupling, we applied Kuramoto model. In this example, phase oscillators distributed randomly at t=0, were allowed to synchronize gradually. Partial synchronicity was mapped by dividing the phase diagram into 43 equal bins (corresponding to 43 temporal bins of 40-min

duration) and calculating the cumulative distribution of nodes in bins with reference to $\theta=2\pi$ (the abstract point of entry into mitosis) in a counter-clockwise direction.

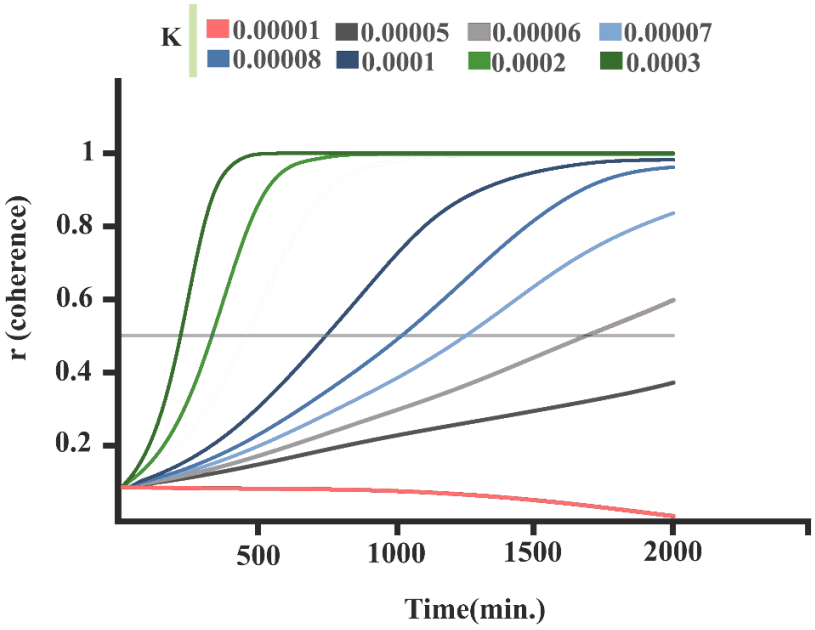

Fig. S4. The order parameter (r) is plotted as a function of time for various values of coupling strength. Note the emergence of partial synchronicity for coupling strength of 0.00005 and 0.00006 after 500-1500 minutes. At higher strength, phase locking precludes the study of emergence of synchronization.

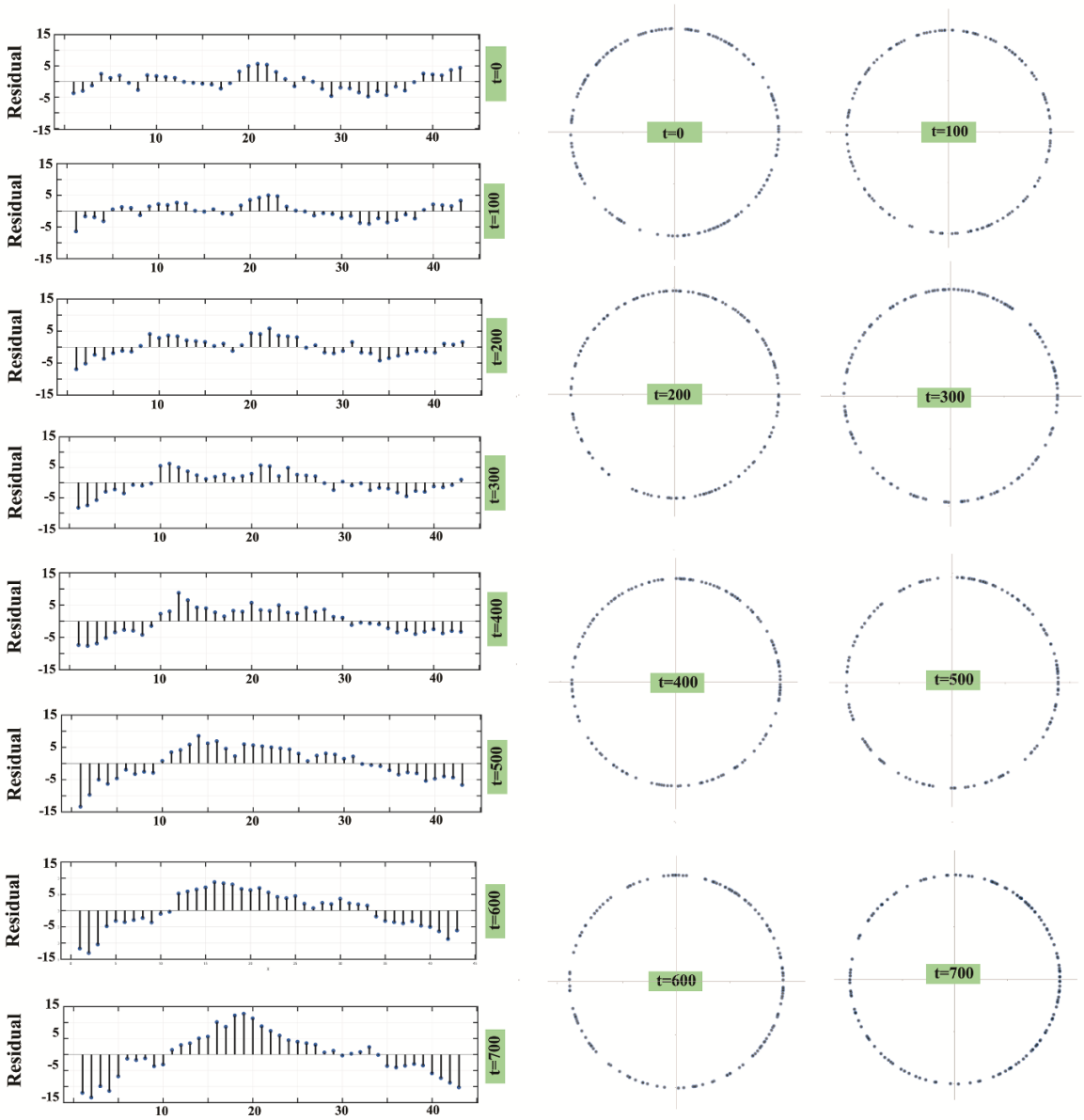

Fig. S5. Emergence of partial synchronicity in Kuramoto model of coupled oscillations. At t=0, random distribution of uncoupled oscillators leads to near-linear cumulative distribution of oscillators in the phase diagram (phase diagram is divided into $2\pi/43$ equal bins). Gradual emergence of partial synchronicity under instruction from a weak couple generates the bottom graph.

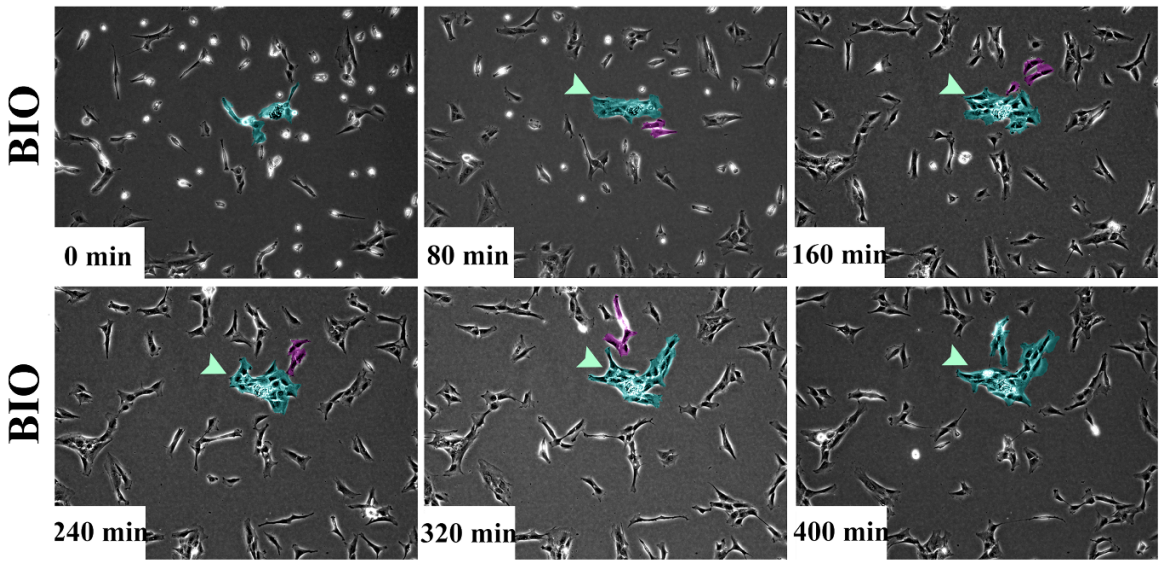

Fig. S6. Migratory behavior of neural progenitor cells subsequent to the application of BIO. Unlike control cell, BIO^{+} cells form cellular clusters (green and purple) and gradually become stationary.

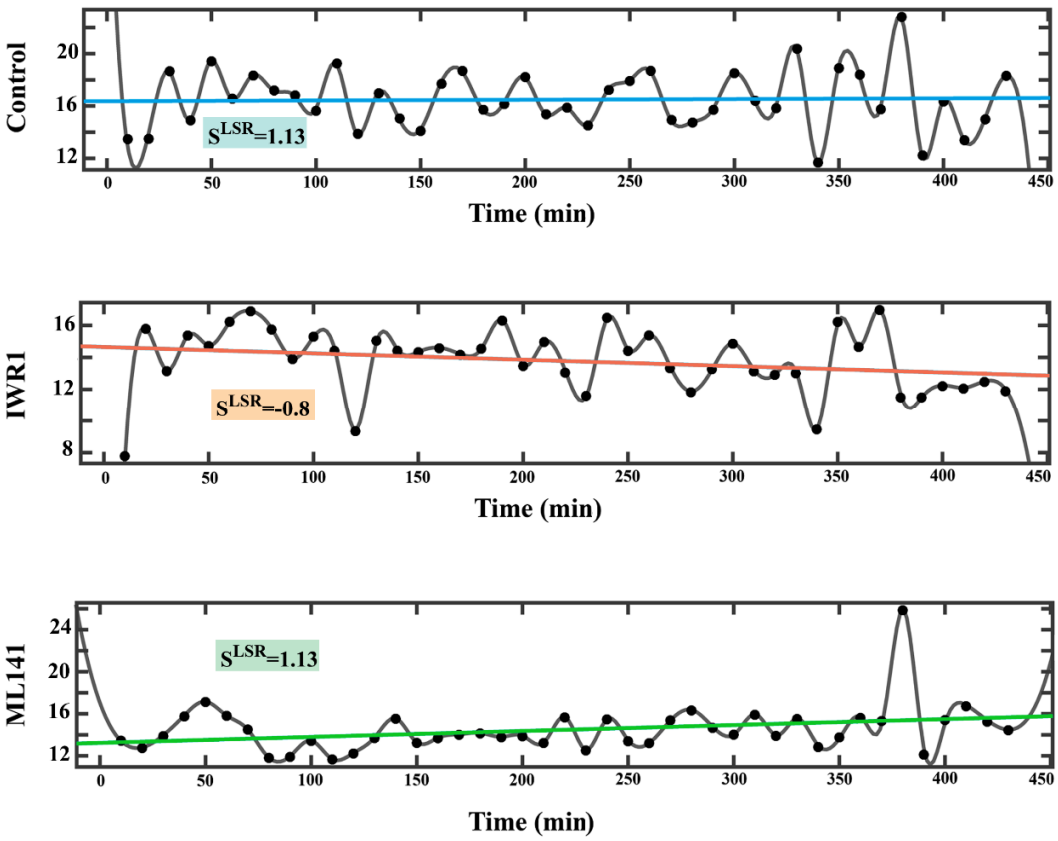

Fig. S7. Average velocity of migratory progenitor cells in coupled and uncoupled states. Graphs demonstrate the averaged migratory velocity of cells at various time points and the slope of the least-squares regression lines (S^{LSR}) indicated the population level tendency to accelerate or decelerate subsequent to the addition of the coupler and the uncoupler. Note that progenitor cells in coupled state (IWR^{+}, 100 nM) tend to decelerate over time (due to amplification of intercellular communications), while the uncoupled cells ($ML141^{+}$, 100 nM) show the opposite trend.

Supplementary Table S1. Transcript-specific primers used in the current study.

Gene	Accession No.	Oligos	Primer sequence	Amplicon size (bps)
TP53	NM_000546.5	F-primer R-primer	GCTCAGATAGCGATGGTCTGGC CTCATAGGGCACCACCACACT	131
CTNNB1-short isoform	NM_001330729.1	F-primer R-primer	TGGCTACTCAAGCTGATTTGATGGAGT ACTCCATCAAATCAGCTTGAGTAGCCA	125
CTNNB1-long isoform	NM_001098209.1	F-primer R-primer	GAAGGTGTGGCGACATATGCAGC AGATCAGCAGTCTCATTCCAAGCCA	143
NOTCH1	NM_017617.4	F-primer R-primer	GCATCTGTGCCAGTACGATGTGG CCGTGTACCCTTCCGTGCA	113
CDH2	NM_001792.4	F-primer R-primer	GAGCTGACCAGCCTCCAACT TGCATGTGCCCTCAAATGAAACCG	116
HES1	NM_005524.3	F-primer R-primer	GGATGCTCTGAAGAAAGATAGCTCGC CGGAGGTGCTTCACTGTCATTTCC	81
HEY1	NM_012258.3	F-primer R-primer	CATACGGCAGGAGGGAAAGGTTAC AAGCGGGTCAGAGGCATCTAGT	138
HEY2	XM_017010629.1	F-primer R-primer	GCAACAGGGGGTAAAGGCTACT AGATGAGACACAAGCCGCACC	158
ACTB	NM_001101.3	F-primer R-primer	AGAGCTACGAGCTGCCTGACG GGACTCCATGCCCAGGAAGGA	101
ATOH1	NM_005172.1	F-primer R-primer	GTGCAGAAGCAGAGACGGCTA GCTCGGACAAGGCGTTGATGTAG	175
MASH1	NM_004316.3	F-primer R-primer	CGGACGAGGGCTCTTACGAC GTGCGATCACCCTGCTTCCA	129
NGN2	NM_024019.3	F-primer R-primer	CGCTGAGGCACAGTTAGAGCC GCTCCTCCTCCTCTTCTTCGTCG	161
snai1	NM_005985.3	F-primer	CGCTCTTTCCTCGTCAGGAA	95

		R-primer	GGCTGCTGGAAGGTAAACTCTGG	
Snai2	NM_003068.4	F-primer R-primer	GCGAACTGGACACACATACAGTGA GCGGTAGTCCACACAGTGATGG	107
twist1	NM_000474.3	F-primer R-primer	GGCCGGAGACCTAGATGTCATTG CCCCACGCCCTGTTTCTTTGA	133

Supplementary movie S1. Live-imaging microscopy of human neural progenitors that express Fucci reporter dye.

Supplementary movie S2. Live-imaging microscopy of human neural progenitors that express Fucci reporter dye.